significantly lower than $R(F) = 0.045$ for the $P2_1/c$ symmetry. The $R(F)$ values for the 152 symmetry-"forbidden" reflections [$(h0l)$, $l = 2n + 1$, and $(0k0)$, $k = 2n + 1$] refined to 0.20; for a true $P2_1/c$ structure this value would be equal to 1. An analogous refinement was performed for sector A. Refinement led to $R(F) = 0.042$ for space group $P2_1/c$ and to $R(F) = 0.040$ for space group $P\bar{1}$. $R(F)$ for the 151 "forbidden" reflections was 0.35.
11. W. C. Hamilton, *Acta Crystallogr.* **18**, 502 (1965).
12. Because of the enantiomorphic relation of sectors A and Ā, the orientations of the surface sites 1, 2, 3, and 4 at face $(0\bar{1}1)$ correspond to surface sites 2, 1, 4, and 3, respectively, at face $(0\bar{1}\bar{1})$.
13. The refined occupancies of the sites 1, 2 and 3, 4 for space group *Pc* were 0.100(1) and 0.039(1), respectively.
14. G. M. J. Schmidt, *Pure Appl. Chem.* **27**, 647 (1971).
15. M. D. Cohen, R. Cohen, M. Lahav, P. L. Nie, *J. Chem. Soc.* **1973**, 1095 (1973). The absolute configurations of these products are currently being determined.
16. L. Addadi *et al.*, *Nature* **296**, 21 (1982).
17. J. L. Wang, Z. Berkovitch-Yellin, L. Leiserowitz, *Acta Crystallogr. Sect. B* **41**, 341 (1985).
18. G. M. Sheldrick, SHELX Program for Crystal Structure Determination, University of Cambridge, Cambridge, 1976.
19. I. Weissbuch, M. Lahav, L. Leiserowitz, G. Meredith, H. van Herzeele, in preparation.
20. We thank L. Addadi and Z. Berkovitch-Yellin for fruitful discussions and M. D. Cohen and F. Hirshfeld for critical readings of this manuscript. This work was supported by the Minerva Foundation and the Israel Academy of Science and Humanities. The neutron diffraction data were measured at Brookhaven National Laboratory under contract DE-AC02-76CH00016 from the U.S. Department of Energy.

14 April 1988; accepted 13 July 1988

$[Cr_4S(O_2CCH_3)_8(H_2O)_4](BF_4)_2 \cdot H_2O$: Ferromagnetically Coupled Cr_4S Cluster with Spin 6 Ground State

A. BINO,* D. C. JOHNSTON,† D. P. GOSHORN, T. R. HALBERT, E. I. STIEFEL

Data on the preparation, structure, and magnetism of the new complex $[Cr_4S(O_2CCH_3)_8(H_2O)_4](BF_4)_2 \cdot H_2O$ are presented. The metal-sulfur M_4S core structure is similar to that found in $M_4S[S_2As(CH_3)_2]_6$ (where M is cobalt or zinc) compounds and in beryllium basic acetate. However, the six-coordinate metal ions in the new Cr_4S system distinguish it from these structures. The tetranuclear chromium complex is the first example of a new structural type. Its magnetic spin $S = 6$ ground state, a striking example of intramolecular ferromagnetic coupling, was determined by variable-temperature magnetic susceptibility measurements. Long-range antiferromagnetic intercluster ordering was found below 170 millikelvin.

INTRAMOLECULAR MAGNETIC COUpling is a phenomenon that has ramifications in physics (*1*), chemistry (*2, 3*), materials science (*4*), biology (*5*), and geology (*6*). Transition-metal cluster compounds containing two or more metal centers provide fertile ground for detailed investigation of such magnetic coupling. Early work on molecular systems recognized only antiferromagnetic coupling (spin pairing), where the magnetic moment of the ensemble of (atomic) paramagnets in the molecule is lowered from the maximally attainable value. In 1968 it was realized (*7*) that ferromagnetic intramolecular coupling is also possible (*8*). The magnetic properties of bi- and trinuclear Cr(III) complexes have been intensely studied (*9*). In trinuclear systems, the basic chromium acetate cation $[Cr_3O(O_2CCH_3)_6(H_2O)_3]^+$ is the prototypical complex for study of antiferromagnetic interactions between the spin $s = 3/2$ Cr(III) ions (*10*). In fact, in di-, tri-, and tetranuclear complexes containing Cr(III), antiferromagnetic coupling is almost invariably found.

We report here a new and unusual tetranuclear sulfur-centered [Cr(III)]$_4$ complex that exhibits intramolecular ferromagnetic coupling with a ground state that has the maximal spin $S = 6$. The compound also exhibits weak intercluster antiferromagnetic interactions, leading to long-range antiferromagnetic ordering of the $S = 6$ clusters in the solid state below 170 mK. Data on the preparation, structure, and magnetism of the new complex, $[Cr_4S(O_2CCH_3)_8(H_2O)_4](BF_4)_2 \cdot H_2O$ (**I**) are presented.

The reaction of chromium metal powder [or $Cr(CO)_6$] with sulfur in refluxing acetic acid : acetic anhydride (1:1) yields a mixture of soluble cationic species composed primarily of the well-known green basic chromium acetate cation and a new blue cation (*11*). The basic chromium acetate can be separated from the blue species by ion-exchange chromatography on Dowex 50W-X2. Elution with 0.1*M* HBF_4 yields the green basic chromium acetate cation. Subsequent elution with 0.5*M* HBF_4 yields the blue cation, which can be crystallized as the BF_4^- salt by evaporation and then recrystallized from methanol (*11*). The visible spectrum is consistent with a Cr(III) complex. Elemental analysis indicates the composition $[Cr_4S(O_2CCH_3)_8(H_2O)_4](BF_4)_2 \cdot H_2O$.

The structure of **I** was solved by single-crystal x-ray diffraction techniques (*12*) (Tables 1 and 2). The structure (Fig. 1) consists of a central four-coordinate sulfur (S) atom bound to four Cr atoms that are in an approximate tetrahedral array. This core is, in a sense, an inverse cluster with the S ligand in the center and the four metal ions on the outside. The Cr-Cr distances average 3.83 Å (range, 3.72 to 3.91 Å). Each Cr atom is six-coordinate with a nearly octahedral arrangement of five oxygen (O) donors and the central S atom. The one water ligand on each Cr lies *trans* to the central S atom. The bridging acetate ligands provide the remaining O atoms bonded to each Cr atom. The overall symmetry of the cation is nearly D_{2d}, whereas that of the inner Cr_4S core is nearly T_d. The structure is related to that of beryllium basic acetate (*13*), $Be_4O(O_2CCH_3)_6$, although in the latter structure the Be atoms are tetrahedrally four-coordinated rather than octahedrally six-coordinated as in the Cr_4S complex. The tetrahedral central S atom is found in $Zn_4S[S_2P(OCH_3)_2]_6$ (*14*) and in the compounds $M_4S[S_2As(CH_3)_2]_6$ (M = Co, Zn) (*15*), which also have the basic beryllium acetate structure. In contrast, the basic chromium acetate cation, $[Cr_3O(O_2CCH_3)_6(H_2O)_3]^+$, has an O atom in the center of an

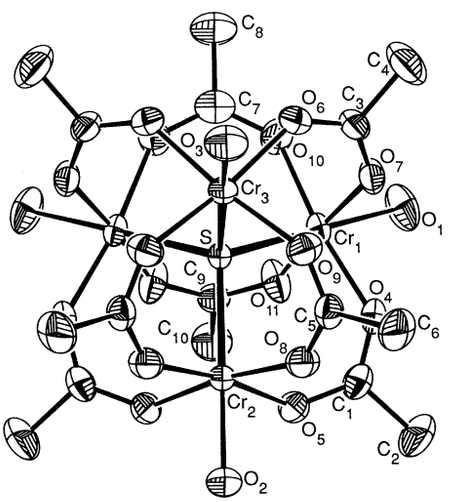

Fig. 1. Perspective drawing of the $[Cr_4S(O_2CCH_3)_8(H_2O)_4]^{2+}$ cation in $[Cr_4S(O_2CCH_3)_8H_2O)_4](BF_4)_2 \cdot H_2O$ with nonhydrogen atoms represented by thermal vibration ellipsoids drawn to encompass 50% of their electron density. Hydrogen atoms are omitted. Unlabeled atoms are related to labeled atoms by the crystallographic mirror plane which contains Cr_2, Cr_3, O_2, O_3, C_7, C_8, C_9, and C_{10}.

Exxon Research and Engineering Company, Annandale, NJ 08801.

*Permanent address: Department of Inorganic and Analytical Chemistry, Hebrew University, Jerusalem, Israel. †Present address: Ames Laboratory–U.S. Department of Energy and Department of Physics, Iowa State University, Ames, IA 50011.

equilateral Cr_3 triangle (*16*).

Complex **I** represents a new structural type containing a central four-coordinated S atom with four octahedrally coordinated metal ions on the tetrahedral periphery. The uniqueness of the new structure notwithstanding, the most unusual feature of **I** is its magnetic behavior. Data on magnetic susceptibility χ versus temperature T were obtained for a polycrystalline sample of **I** between 4 and 300 K in a magnetic field H of 6.3 kG. The $\chi(T)$ data are corrected for the contribution of ferromagnetic impurities and for the core diamagnetism, calculated to be $\chi_0 = -4.66 \times 10^{-4}$ cm^3 per mole of Cr_4. The shape of the inverse of χ corrected for χ_0, $(\chi - \chi_0)^{-1}$, versus T (Fig. 2) is unusual for a cluster compound, indicating ferromagnetic intracluster interactions, as follows. A Curie law straight-line fit ($\chi = C/T$) to the lowest T data, which are linear in T ($0 \leq T \leq 50$ K) in Fig. 2 (dashed line), yields the Curie constant $C = 21.3 \pm 0.2$ (SE) cm^3-K per mole of Cr_4, where

$$C = Ng^2S(S + 1)\mu_B^2/3k_B$$

(N is Avogadro's number, g is the Landé g factor for the Cr^{3+} ion, S is the spin of the Cr_4 cluster, μ_B is the Bohr magneton, and k_B is Boltzmann's constant). The effective moment per cluster is $\mu_{eff} = g[S(S+1)]^{1/2}\ \mu_B = 13.05\ \mu_B$. Assuming $g = 2$ (substantiated below), we find $S = 6$ for the ground state of the Cr_4 cluster from the value of C or μ_{eff} found above. Because each Cr^{3+} ion in the cluster has spin $s = 3/2$, the spins of the four Cr^{3+} ions must be ferromagnetically aligned in the ground state of the Cr_4 cluster.

Magnetization data, obtained up to 40 kG at 1.27 and 4.22 K in a vibrating sample magnetometer, are plotted versus reduced field $\mu_B H/k_B(T - \theta)$ in Fig. 3, where $\theta = -0.4$ K is the Weiss temperature found from $\chi(T)$ data between 1.27 and 4.22 K; the data for the two temperatures lie on a common curve. The high-field saturation moment $M^{sat} = gS\mu_B$ is equal to 12.0 ± 0.1 (SE) μ_B per cluster. With the above value of μ_{eff}, these two measurements together prove that $S = 6$ with $g \simeq 2$: we find $g = 2.00 \pm 0.02$ (SE). Also plotted in Fig. 3 are Brillouin functions for $S = 6$ and $S = 3/2$ with $M^{sat} = 12\ \mu_B$ per cluster and $g = 2$ in both cases. The curve for $S = 6$ fits the data quite well, in contrast to the curve for $S = 3/2$, which would be obtained if the four Cr atoms in each cluster were magnetically isolated from each other.

Static $\chi(T)$ data at 75 G were obtained for the same powder sample as in Figs. 2 and 3 between 13 mK and 1.2 K using a superconducting quantum interference device (SQUID) magnetometer. Plots of $\chi(T)$ and its inverse (Fig. 4, a and b) show that long-range antiferromagnetic intercluster ordering occurs below about 190 mK. The actual Néel temperature T_N is that at which $d\chi/dT$ attains a maximum, $T_N \simeq 170$ mK. The positive deviation of the data in Fig. 4b from Curie-Weiss behavior (straight line) between T_N and 700 mK is probably caused by the onset of short-range antiferromagnetic intercluster ordering. The Weiss temperature from Fig. 4b obtained by fitting to the data between 0.7 and 1.2 K is $\theta = -307$ mK, antiferromagnetic in sign and similar in magnitude to T_N.

We turn now to an analysis of the susceptibility data above 50 K in Fig. 2. Because the four Cr atoms per Cr_4 cluster form a nearly perfect tetrahedron, we analyze the data in Fig. 2 in terms of a model in which the strengths of all the Cr-Cr exchange interactions within the cluster are the same and isotropic (Heisenberg-like). The Hamiltonian is then (*17*)

$$\mathcal{H} = -2J \sum_{j>i=1}^{4} \mathbf{s}_i \cdot \mathbf{s}_j \qquad (1)$$

where $s = 3/2$ is the spin of Cr^{3+}, and J is the coupling constant. Equation 1 is easily diagonalized, yielding the energy eigenvalues $E_S = -JS(S + 1)$, where $S = 0, 1, \ldots, 6$. The magnetic susceptibility per mole of Cr_4 clusters is

$$\chi = \frac{Ng^2\mu_B^2}{3Zk_BT} \times \sum_{S=0}^{6} G_S S(S + 1)\ (2S + 1)e^{-E_S/k_BT} \qquad (2a)$$

where G_S is the degeneracy of the levels at energy E_S, not including the Zeeman degeneracy, and the partition function Z is

$$Z = \sum_{S=0}^{6} G_S(2S + 1)e^{-E_S/k_BT} \qquad (2b)$$

One obtains the G_S values using the rule for addition of angular momenta, yielding

Table 1. Key bond lengths and polyhedral edge lengths in crystalline $[Cr_4S(O_2CCH_3)_8(H_2O)_4](BF_4)_2 \cdot H_2O$. The numbers in parentheses are the estimated standard deviations in the last significant digit and are computed by the Nicolet SHELXTAL program. Primed (′) atoms are related to nonprimed atoms by a crystallographic mirror plane. Atoms are labeled in agreement with Fig. 1 (primed atoms are unlabeled in the figure).

Type	Length (Å)
Bond	
Cr_1–S	2.347(1)
Cr_2–S	2.349(2)
Cr_3–S	2.351(2)
Cr_1–O_1	2.034(3)
Cr_2–O_2	2.031(6)
Cr_3–O_3	2.026(6)
Cr_2–O_5	1.959(3)
Cr_2–O_8	1.946(3)
Cr_1–O_4	1.962(3)
Cr_1–O_{10}	1.949(3)
Cr_1–O_7	1.953(3)
Cr_1–O_{11}	1.946(3)
Cr_3–O_6	1.967(3)
Cr_3–O_9	1.959(3)
Polyhedral edge	
$Cr_1 \ldots Cr_1'$	3.716(1)
$Cr_1 \ldots Cr_2$	3.874(1)
$Cr_1 \ldots Cr_3$	3.910(1)
$Cr_2 \ldots Cr_3$	3.720(1)

Table 2. Selected bond angles for the cation in crystalline $[Cr_4S(O_2CCH_3)_8(H_2O)_4](BF_4)_2 \cdot H_2O$ (see Table 1 for explanation of entries).

Type	Angle
Cr_1–S–Cr_2	111.2(1)
Cr_2–S–Cr_3	104.7(1)
Cr_1–S–Cr_3	112.7(1)
Cr_1–S–Cr_1'	104.7(1)

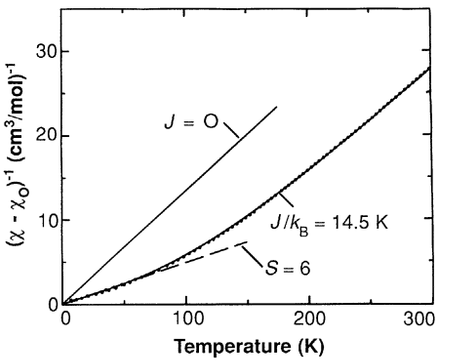

Fig. 2. Inverse molar magnetic susceptibility $(\chi - \chi_0)^{-1}$ versus temperature for $[Cr_4S(O_2CCH_3)_8(H_2O)_4](BF_4)_2 \cdot H_2O$. The solid curve through the data points is a theoretical fit, the solid straight line is the behavior expected for isolated Cr(III) ions, and the dashed line is a straight-line fit to the data below 50 K.

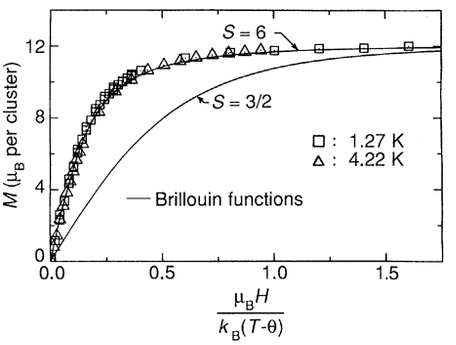

Fig. 3. Magnetization M per Cr_4 cluster versus reduced magnetic field $\mu_B H/k_B(T - \theta)$ for $[Cr_4S(O_2CCH_3)_8(H_2O)_4](BF_4)_2 \cdot H_2O$ at 1.27 and 4.22 K in fields up to 40 kG. The solid curves are Brillouin functions for $S = 6$ and $S = 3/2$, both with saturation magnetizations of 12.0 μ_B per cluster and $g = 2$.

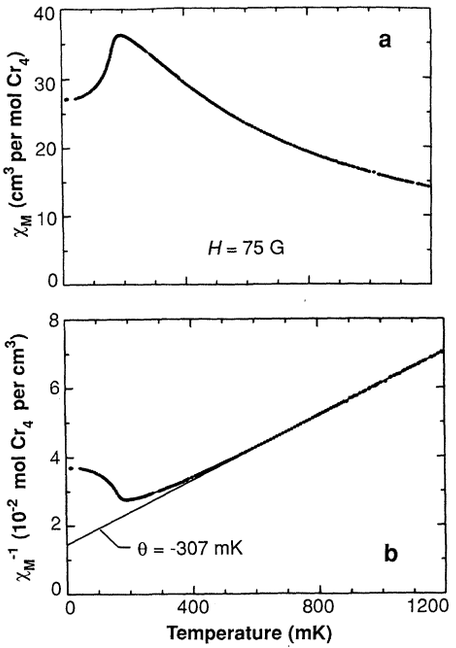

Fig. 4. The dc molar magnetic susceptibility (**a**) and its inverse (**b**) versus temperature for $[Cr_4S(O_2CCH_3)_8(H_2O)_4](BF_4)_2 \cdot H_2O$ between 13 mK and 1.2 K. The data have been normalized to the data in Fig. 2 above 1 K.

G_S = 4, 9, 11, 10, 6, 3, and 1 for S = 0, 1, . . .,6, respectively. An excellent single-parameter fit of Eq. 2 to the data in Fig. 2 was obtained for $J/k_B = +14.5 \pm 0.3$ K (ferromagnetic intracluster interactions) and $g = 2$, as shown by the solid curve through the data in Fig. 2. This agreement strongly supports the original assumptions that the strengths of the Cr-Cr intracluster exchange interactions are all about the same and are Heisenberg-like.

The electron paramagnetic resonance spectrum at 15 K of **I** dissolved and frozen in methanol shows a single broad peak with $g = 1.983$ and peak-to-peak width of 160 G. The g value is approximately that found from the magnetic studies on the solid compound.

The 12 unpaired electrons in the relatively small $[Cr_4S(O_2CCH_3)_8(H_2O)_4]^{2+}$ ion suggest many potential uses. The complex cation could be used as a contrasting agent for nuclear magnetic resonance (NMR) imaging or as a zero-shift relaxation reagent to aid the accumulation of ^{13}C NMR data. The water ligands on **I** are potentially labile, making it possible to bind this cation to a ligand on a protein or other macromolecule. As such a spin label, its magnetic effect on neighboring nuclei would reveal its location. Attaching the tetranuclear Cr_4S unit to a polymer would allow its strong paramagnetism to be exploited by using a magnetic field to orient the cluster and the attached polymer. The cluster could also be useful as a selective microwave absorber that could, in a magnetic field, facilitate localized heating in a particular organelle, organ, organism, or inanimate substructure. Moreover, the cation could be used as part of a thermometer for measurements above 0.2 K.

REFERENCES AND NOTES

1. K. Kambe, *J. Phys. Soc. Jpn.* **5**, 48 (1950); J. H. Van Vleck, *Science* **201**, 113 (1978).
2. R. L. Carlin, *Magnetochemistry* (Springer-Verlag, New York, 1985).
3. R. D. Willett, D. Gatteschi, O. Kahn, Eds., *Magneto-Structural Correlations in Exchange Coupled Systems* (Reidel, Dordrecht, 1985).
4. J. B. Goodenough, *Magnetism and the Chemical Bond* (Wiley, New York, 1966).
5. E. I. Solomon and D. E. Wilcox, in (*3*), p. 463.
6. D. J. Vaughan and J. R. Craig, *Mineral Chemistry of Metal Sulfides* (Cambridge Univ. Press, New York, 1978).
7. A. P. Ginsberg, R. L. Martin, R. C. Sherwood, *Inorg. Chem.* 7, 932 (1968).
8. C. J. Cairus and D. H. Buscel, *Coord. Chem. Rev.* **69**, 1 (1986).
9. D. J. Hodgson, in (*3*), p. 497.
10. B. S. Tsukerblat, M. I. Belinskii, B. Ya. Kuyavskaya, *Inorg. Chem.* **22**, 995 (1983), and references therein.
11. The $[Cr_4S(O_2CCH_3)_8(H_2O)_4](BF_4)_2 \cdot H_2O$ was prepared as follows: Cr metal (−100 mesh powder, 0.5 g, 9.6 mmol) and elemental S (0.6 g, 18.8 mmol) were added to 50 ml of a 1:1 mixture of acetic acid:acetic anhydride in a 100-ml flask equipped with a condenser. The flask was placed in an oil bath that had been preheated to 147° ± 1°C, and the mixture was stirred vigorously for 3.5 hours. The resulting blue-green solution was poured (while still hot) into 200 ml of cold water and mixed thoroughly. After standing for 3 hours the white precipitate was separated by filtration through a bed of kieselgühr on a medium-porosity sintered glass funnel. The filtrate was adsorbed on a Dowex 50W-X2 cation-exchange column (15 by 45 mm). After the precipitate was washed with several volumes of water, elution with 0.1*M* HBF_4 solution removed a green band of $[Cr_3O(O_2CCH_3)_6(H_2O)_3]^+$. The blue band of $[Cr_4S(O_2CCH_3)_8(H_2O)_4]^{2+}$ was then removed with 0.5*M* HBF_4, and the blue solution was placed in a desiccator for evaporation. When the volume was reduced to about 1 ml, the mixture of blue crystals and white powder was filtered and washed with ether. The solid mixture in the filter was extracted three times with methanol (4 ml each time). Evaporation of the combined dark blue methanol extracts gave 472 mg of $[Cr_4S(O_2CCH_3)_8(H_2O)_4](BF_4)_2 \cdot H_2O$ as well-formed dark blue crystals (yield: 20% based on Cr metal). The ultraviolet-visible spectrum of **I** in H_2O yields the following data in the form $\lambda(\epsilon)$, where λ is wavelength in nanometers and ϵ is the molar extinction coefficient in mol^{-1} cm^{-1}: 705(76)sh, 605(540), 490(54)sh, 442(147), 325(1000)sh (sh, shoulder). Elemental analysis calculated for $Cr_4SF_8O_{21}C_{16}B_2H_{34}$ (percent by weight): C, 19.67; H, 3.48; S, 3.28; Cr, 21.31; F, 15.57. Composition found: C, 18.93; H, 3.46; S, 3.50; Cr, 20.48; F, 15.39.
12. Complex **I** crystallizes in space group *Pnma* (number 62) with a = 21.006(4) Å, b = 19.086(3) Å, and c = 9.323(1) Å (numbers in parentheses are standard deviations in the last digit). The structure was solved by a combination of direct methods and difference Fourier syntheses, and refined to a final R factor of 0.048. We acknowledge the contribution of C. Day, Crystalytics Company, in the solution of the structure. The atomic coordinates for this work are available on request from the Director of the Cambridge Crystallographic Data Centre, University Chemical Laboratory, Lensfield Road, Cambridge, CB2 1EW, England. Any request should be accompanied by the full literature citation for this communication.
13. W. H. Bragg and C. T. Moran, *Proc. R. Soc. London Ser. A* **104**, 437 (1923).
14. A. J. Burn and G. W. Smith, *Chem. Commun.* **1965**, 394 (1965).
15. D. Johnstone, J. E. Fergusson, W. I. Robinson, *Bull. Chem. Soc. Jpn.* **45**, 3721 (1972).
16. S. C. Chang and G. A. Jeffrey, *Acta Crystallogr. Sect. B* **26**, 673 (1970).
17. For a lucid review of the theory see E. Sinn, *Coord. Chem. Rev.* **5**, 313 (1970).

31 March 1988; accepted 18 July 1988

Nef Protein of HIV-1 Is a Transcriptional Repressor of HIV-1 LTR

NAFEES AHMAD AND SUNDARARAJAN VENKATESAN*

In studies of the genetics of human immunodeficiency virus type 1 (HIV-1), the product of the *nef* gene, formerly known as F, 3′-*orf*, or B-ORF, was a negative regulator of HIV-1 replication. Proviruses with mutations in the *nef* gene replicated better than their standard counterparts during transient expression, and the mutant virus maintained its enhanced replication even after serial passages in T lymphocytes. The *nef* protein trans-suppressed, in a dose-dependent manner, the replication of wild-type and *nef* mutant proviruses and the expression of reporter genes linked to the HIV-1 long terminal repeat (LTR). The repression induced by the *nef* protein was mediated by inhibition of transcription from the HIV-1 LTR, which contains a far upstream cis element (previously recognized to be a negative regulatory element) between 340 and 156 nucleotides upstream of the RNA initiation site.

THE BASAL TRANSCRIPTION OF HIV-1 is governed by the interactions of several cis-acting elements in the HIV-1 LTR with cellular transcriptional factors such as TATAA, SP1, and NFκB factors (*1*). Replication of the virus is dependent on the functional expression of certain small virus-coded regulatory proteins, such as the *tat* gene product (Tat) of 86 amino

Laboratory of Molecular Microbiology, National Institute of Allergy and Infectious Diseases, National Institutes of Health, Bethesda, MD 20892.

*To whom correspondence should be addressed.